Numerical study of substrate assimilation by a microorganism exposed to fluctuating concentration

Marion Linkès, Marco Martins Afonso, Pascal Fede, Jérôme Morchain, Philippe Schmitz

Numerical study of substrate assimilation by a microorganism exposed to fluctuating concentration

Marion Linkès [a,b,*], Marco Martins Afonso [a,b,d], Pascal Fede [a,b], Jérôme Morchain [c], Philippe Schmitz [c]

[a] CNRS, IMFT, allée du Professeur Camille Soula, 31400 Toulouse, France
[b] Université de Toulouse, INP/UPS/IMFT, allée du Professeur Camille Soula, 31400 Toulouse, France
[c] Université de Toulouse, Laboratoire d'Ingénierie des Systèmes Biologiques et des Procédés, INSA/CNRS/INRA, 135 avenue de Rangueil, 31077 Toulouse cedex, France
[d] I3M, CNRS, Université de Montpellier 2, c.c.051, 34095 Montpellier cedex 5, France

Keywords:
Biological engineering
Bioreactors
Numerical analysis
Diffusion
Transport processes
Simulation

A B S T R A C T

In most modelling works on bioreactors, the substrate assimilation is computed from the volume average concentration. The possible occurrence of a competition between the transport of substrate towards the cell and the assimilation at the cell level is generally overlooked. In order to examine the consequences of such a competition, a diffusion equation for the substrate is coupled with a specific boundary condition defining the uptake rate at the cell–liquid interface. Two assimilation laws are investigated, whereas the concentration far from the cell is varied in order to mimic concentration fluctuations. Both steady and unsteady conditions are investigated. The actual uptake rate computed from the interfacial concentration is compared to the time-averaged uptake rate based on the mean far-field concentration. Whatever the assimilation law, it is found that the uptake rate can be correlated to the mean far-field concentration, but the actual values of the parameters are affected in case of transport limitation. Moreover, the structure of the far-field signal influences the substrate assimilation by the microorganism, and the mean interfacial uptake rate depends on the ratio between the characteristic time of the signal and the diffusional time scale, as well as on the amplitude of the fluctuations around the mean far-field concentration in substrate. The present work enlightens some experimental results and helps in understanding the differences between the concentration measured and that present in the microenvironment of the cells.

1. Introduction

Scale-up problems are frequent in fed-batch bioreactors when passing from a laboratory (~ 1 L) to an industrial scale (~ 10 m^3). It is therefore crucial to understand the reasons for the often observed reduced conversion yield of substrate into biomass, with by-product formation (Larsson et al., 1996; Bylund et al., 1998). One of the first studies of the effect of mixing on microbial behaviour was addressed by Hansford and Humphrey (1966) for Baker's yeast. These degraded performances are attributed to the presence of concentration gradients of substrate, pH and/or oxygen within the reactor. In a fluctuating environment, cells may be unable to adapt dynamically to the local environment and their behaviour thus deviates from that identified at the laboratory scale, i.e. in a steady and homogeneous environment. As pointed out by Enfors et al. (2001) and later by Lara et al. (2006), the behaviour of microorganisms is an integrated consequence of all the fluctuations experienced during their transport within the bioreactor. The difficulty in predicting the changes during

* Corresponding author at: Université de Toulouse, INP/UPS/IMFT, allée du Professeur Camille Soula, 31400 Toulouse, France. Tel.: +33 534322925.
E-mail address: marion.linkes@imft.fr (M. Linkès).

scale-up of fermentations is related to the variety of strongly coupled phenomena such as hydrodynamics, two-phase mass transfer and biological reaction. Beside the experimental approach, the modelling and simulation of bioreactors have been developed; a full integration of the most influential phenomena in a commercial Computational Fluid Dynamics code is possible whilst rare (Schmalzriedt et al., 2003). Unfortunately, the results are somewhat disappointing despite the use of well-established models in each domain of concern. In most cases, the macroscopic gradients at the reactor scale and the amount of by-products are underestimated (Enfors et al., 2001; Schmalzriedt et al., 2003), whereas the biomass production is overestimated.

In many modelling works on bioreactors, the specific substrate uptake rate q_S (grams of substrate by unit of time and cell mass, $g_S\, g_X^{-1}\, s^{-1}$) is modelled using a Monod equation based on the average concentration $\langle S \rangle$. The symbols $\langle \cdot \rangle$ represent a spatial averaging over a volume of control on which mass balances are written. This volume of control can be either the whole reactor if an ideal reactor approach is used, or a portion of the reactor if a compartment model or a CFD approach is used

$$\langle q_S \rangle = q_{max} \frac{\langle S \rangle}{K_S + \langle S \rangle} \tag{1}$$

q_{max} is defined as the maximum specific uptake rate and K_S is the affinity constant for the substrate.

Based on zone models, several studies focused on the macro-mixing issues for bioreactors. Bajpai and Reuss (1982) investigated the effect of dynamical effect of the mixing process in mechanically stirred bioreactors by using a circulation model for the fluid flow and a two-environment model to account for micro-mixing in the vessel. The biological reaction obeys a kinetic model. They obtained a circulation time distribution which is more a macro-mixing issue. Namdev et al. (1992) also studied the circulation time distribution. They evaluated the effects of the feed zone by conducting aerobic fed-batch fermentations of *Saccharomyses cerevisiae* with a recycle loop and a bench-scale fermentor. The intermittent feed in the recycle loop simulates the circulation of cells through the feed zone for different residence times, and the biomass yield is increased in the feed zone for long-time exposure. Considering zone models, those works assume that the micro-mixing is perfect, because they consider a homogeneous concentration $\langle S \rangle$ in the zone. Recent works from Garcia et al. (2009) reveal that oxygen limitations are actually experienced whereas bulk oxygen concentration is non-limiting. This suggests the existence of micro-mixing issues in well macro-mixed laboratory-scale bioreactors.

In these approaches, all species are treated as dissolved species, but as far as microbial populations are considered, it might be more meaningful to make an analogy with heterogeneous catalysis considering suspended particles in a liquid phase.

Therefore, two asymptotic regimes can be distinguished: the biological regime if the transport rate towards the particle is larger than the reaction rate, and the physical regime if it is smaller. Experimental evidences of assimilation taking place in the physical regime have been given by Hondzo and Al-Homoud (2007). These authors showed that, at a very low dissipation rate ($7 \times 10^{-6} \leq \varepsilon \leq 180 \times 10^{-6}$, ε dissipation rate in $m^2\, s^{-3}$), the oxygen uptake rate is correlated to the energy dissipation rate and therefore controlled by the rate of transport towards the cell surface. From the cell position, the competition between transport towards the cell and substrate assimilation results in a heterogeneous concentration field: the concentration at the cell surface differs from the average concentration $\langle S \rangle$. The latter is sometimes referred as the bulk concentration or far-field concentration (concentration far from the cell).

In the classical approach, the substrate concentrations are treated as spatial or temporal averages. The present work focuses on dynamic simulations where the influence of temporal fluctuations of the substrate concentration on the assimilation by one microorganism is scrutinised. These temporal evolutions can be thought as the different substrate concentration experienced by a microorganism transported in a bioreactor. The assimilation is of prime interest and requires a precise modelling.

From a biological point of view, assimilation has been studied by Koch and Houston Wang (1982), Ferenci (1996), Natarajan and Srienc (1999, 2000), Lin et al. (2001) and Chassagnole et al. (2002), among others. One important conclusion concerns the ability of cells to modify their assimilation capacity in response to the concentration fluctuations encountered. Without ignoring these particular features of biological systems, only the physical aspects of the problem will be considered in this paper, and no adaptation or regulation of the uptake systems is taken into account. In other words, the parameters of the assimilation law, q_{max} and K_S, will be regarded as pure constants.

The originality of the work concerns the microscopic description of the assimilation at the microorganism's interface. The uptake rate is based on local quantities, such as the interfacial concentration that is different from the bulk concentration, and this results in a competition between transport and assimilation.

As a first step, we propose to investigate the case where the substrate transport towards the cell is controlled by a molecular diffusion process. The aim of this work is to scrutinise the influence of a time-varying far-field concentration on both the interfacial concentration and assimilation rate dynamics at the cell scale. This question is addressed through the resolution of a scalar diffusion equation in spherical coordinates. The analytical resolution for such a problem is known for some particular boundary conditions (Truskey et al., 2004) and used to validate the tool. Then, a numerical resolution with various boundary conditions at the cell surface is performed, allowing the calculation of both the interfacial flux and concentration under transient conditions. First, an assimilation law based on a Monod equation is used. It is shown that it is not possible to correlate the mean assimilation rate to the mean far-field concentration without adapting the constant of the assimilation law. We propose an alternative bi-linear formulation of the assimilation law that reproduces the asymptotic behaviours (biological and physical regimes). This model is applied under transient conditions and the influence of different parameters of the concentration field on the assimilation rate is enlightened. At steady state, the interfacial concentration can be obtained by equating the reaction rate to the mass transport rate, and an overall reaction rate can be expressed as a function of the bulk concentration. Under transient conditions, the elimination of the unknown interfacial concentration is no longer possible, and the full set of partial-differential equations for scalar transport and assimilation at the particle has to be considered.

Using this procedure, it is shown that the microorganism will be exposed to highly substrate-limited events whereas the bulk concentration is highly non-limiting.

2. Model framework

2.1. Geometry and boundary conditions

The computational domain can be seen as a sphere of stagnant fluid, and the microorganism, spherical as well, is located at its centre. The external boundary of the domain, indicated by a long-dashed line in Fig. 1, is homogeneously supplied in substrate with the concentration S_∞, while the short-dashed line represents the

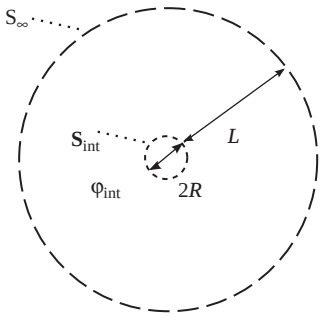

Fig. 1. Configuration of the calculations.

microorganism interface. The scalar transport towards the cell is purely diffusive and follows the spherical diffusion equation. In view of the present geometry and the homogeneous distribution of concentration at the domain boundaries, the concentration is the same all over the cell surface, then the radial component of the equation is sufficient for solving the substrate transport in a satisfactory manner. The diffusion equation in the radial coordinate r, $R \le r \le L$, yields

$$\frac{\partial S}{\partial t} = \frac{\mathcal{D}}{r^2}\frac{\partial}{\partial r}\left(r^2 \frac{\partial S}{\partial r}\right), \tag{2}$$

where S is the substrate concentration in the domain, $\mathcal{D}$ is the molecular diffusivity, R is the microorganism radius which is set constant[1] and L is the length of the domain (large compared to R).[2] Three typical boundary conditions associated to Eq. (2) are investigated in the present work:

- imposed time-varying far-field concentration
$$S_{r=L} = S_\infty(t), \tag{3}$$
- Neumann boundary condition: specified flux at the cell–liquid interface
$$\left.\frac{\partial S}{\partial r}\right|_{r=R} = \varphi_{int}, \tag{4}$$
- Dirichlet boundary condition: specified concentration at the cell–liquid interface
$$S_{int} = S_{r=R} = C. \tag{5}$$

If a Neumann boundary condition along with a Monod assimilation law is chosen, the uptake rate depends on the substrate concentration at the cell–liquid interface and one actually gets $\varphi_{int} = \varphi_{int}(S_{r=R})$. Note that boundary conditions (4) and (5) are mutually exclusive, but can be used to reproduce the asymptotic behaviour of substrate assimilation at high and very low concentrations.

As already mentioned, whatever the actual phenomena ensuring the passage of the substrate through the cell membrane, the latter is preceded by the transport of the substrate to the cell–liquid interface. These two phenomena occur in series and two asymptotic regimes can then be distinguished. On the one hand, when the transport of substrate towards the cell governs the process, typically when the microorganism grows in a nutrient-limited culture, the physical regime stands and the actual uptake rate is indeed limited by the transport rate. The interfacial concentration tends to zero $S_{r=R} \mapsto 0$ which can be translated in terms of boundary conditions by $C=0$ in Eq. (5). On the other hand, in the biological regime the uptake rate is slower than the transport rate and the transfer through the membrane controls the process. This situation typically occurs at high substrate concentration and results in a saturated assimilation capacity. Here, the corresponding boundary conditions are a constant gradient at the cell surface such that the specific uptake rate, q_S, is maximum. The relationships between concentration gradients, mass fluxes and uptake rates are detailed in Section 2.4.

2.2. Numerical framework

Eq. (2) can be spatially discretised in various ways. In order to be as consistent as possible, a conservative form was used, rewriting the radial diffusion equation as

$$\frac{\partial S}{\partial t} = \mathrm{div}(\mathcal{D}\,\mathbf{grad}\,S) \tag{6}$$

This form allows to keep the operator $\mathrm{div}(\mathcal{D}\,\mathbf{grad}\,.)$ in the discretisation, and the interfacial gradient $\varphi_{int} = \partial S/\partial r|_{r=R}$ then appears directly and does not have to be recalculated from the concentration field. This formulation simplifies the imposition of a given flux boundary condition (Neumann boundary condition). Further information on the discretisation can be found out in the Appendix. A first-order implicit time integration was employed for the temporal resolution of the problem. Higher-order temporal schemes have been tested with no significant impact on the results.

2.3. Analytical solutions

Steady-state analytical solutions of Eq. (6) are known for various boundary conditions. Only that of interest, obtained with two Dirichlet boundary conditions, will be reported here. Let S_∞ be the constant concentration at $r = L+R$ and $C=0$ so that the concentration at the cell surface $r=R$ is null, then the steady-state solution of the problem is given by

$$S(r) = S_\infty\left(1+\frac{R}{L}\right)\left(1-\frac{R}{r}\right). \tag{7}$$

The concentration gradient at the cell–liquid interface is

$$\varphi_{int} = \left.\frac{\partial S}{\partial r}\right|_{r=R} = \frac{S_\infty}{R}\left(1+\frac{R}{L}\right). \tag{8}$$

If $L \gg R$ the above expression simplifies into the following:

$$\varphi_{int} \approx \frac{S_\infty}{R} \tag{9}$$

The result of Eq. (9) shows that the concentration gradient at the cell surface can be, in some particular conditions ($S_{r=R} = 0$), independent of the actual length of the domain, provided that the latter is much larger than the cell radius.

An analytical solution can also be found for the unsteady case if one considers a Dirichlet boundary condition, S_∞ at $r = L+R$, a Neumann boundary condition , $\partial S/\partial r|_{r=0} = 0$, and a uniform initial condition, $S(r,0) = 0$ (Truskey et al., 2004):

$$S(r,t) = S_\infty + 2S_\infty\left(2\sum_{n=1}^{\infty}(-1)^n \frac{\sin(n\pi r/L)}{n\pi r/L}\exp^{-n^2\pi^2 t\mathcal{D}/L^2}\right) \tag{10}$$

[1] Notice that, in general, the microorganism can grow up to a mass, i.e. to a volume, which is about the double of its initial value, and then usually subdivides into two cells. The maximum cell diameter or radius attained is thus of the order of $\sqrt[3]{2} \simeq 1.26$ times the initial value, therefore it can be considered as constant with a good approximation.

[2] The length of the domain is important because the substrate is carried on this length. A direct influence of L can be found on the characteristic transport rate. The chosen length L is large compared to R but remains small enough to consider characteristic times of order 20 s.

In our case, the Neumann boundary condition is not imposed at $r=0$ but at $r=R$; nevertheless, if $L \gg R$, the analytical solution above will provide a good approximation of the concentration profile in the early step of the process. It will be used as a reference to test our model under transient conditions. In Eq. (10), the length of the domain L appears explicitly in the characteristic time $\tau_{\mathcal{D}} = L^2/\mathcal{D}$. As such it impacts the dynamics of the scalar transport, but has no impact on the concentration profile $S(r/L,t) = f(t/\tau_{\mathcal{D}})$. The scalar transport dynamics is indeed controlled by the characteristic time rather than by the length of the domain L. Provided that the latter is large compared to the cell radius, numerical solutions should be independent of L and can be compared to analytical solutions. Under transient conditions (time-varying far-field concentration) a key parameter will be the ratio of the concentration fluctuation time scale to the transport time scale $\tau_{\mathcal{D}}$.

2.4. Relating concentration gradient to biological constants

The substrate assimilation is generally defined by a specific uptake rate, in $g_S\ g_X^{-1}\ s^{-1}$, which can also be regarded as a mass flux through the cell membrane, q_{int}, per unit cell mass. This quantity is upper bounded since the cell has a maximum uptake capacity. In practice, the maximum specific uptake rate for a given substrate q_{max} is deduced from experiments

$$q_{max} = \frac{\mu_{max}}{Y_{XS}} \tag{11}$$

where μ_{max} is the maximum specific growth rate of the microorganism and Y_{XS} is a conversion yield of substrate into biomass. The interfacial mass flux Φ_{int} is the equivalent mass of substrate assimilated per unit time. The related maximum mass flux is

$$\Phi_{max} = m_c q_{max} \tag{12}$$

where m_c is the cell mass.

Finally, if one assumes that the transfer through the membrane is uniform over the cell surface, the concentration gradient at the cell surface φ_{int} can be introduced via the relation:

$$\Phi_{int} = a_c \mathcal{D} \varphi_{int} \tag{13}$$

where a_c is the cell surface. The maximum concentration gradient at the microorganism interface corresponding to the saturation of the uptake capacity is thus given by φ_{max}

$$\Phi_{max} = a_c \mathcal{D} \varphi_{max} \tag{14}$$

In the following, the different interfacial quantities are non-dimensionalized by the corresponding above-mentioned maximum interfacial values (see Table 1) and we underlined that the following ratios are equivalent:

$$\frac{\varphi_{int}}{\varphi_{max}} = \frac{q_{int}}{q_{max}} = \frac{\Phi_{int}}{\Phi_{max}} \tag{15}$$

As far as boundary conditions are expressed in terms of concentration gradients, the first ratio of Eq. (15) will be used to present the results in the present work.

Tables 1 and 2 summarise the different biological and physical parameters for the forthcoming calculations.

Table 1
Reference parameters for biological condition.

Y_{XS}	μ^*_{max}	q_{max}	ρ_{cell}	Φ^*_{max}	φ_{max}
0.5	0.6[a]	0.33	1000	1.4×10^{-18}	223
$g_X\ g_S$	h^{-1}	$g_S\ g_X^{-1}\ s^{-1}$	$g_X\ L^{-1}$	$kg_S\ s$	$kg_S\ m^{-4}$

[a] From Lendenmann and Egli (1998).

Table 2
Reference parameters.

R^*	L^*	$\mathcal{D}^*$
10^{-6} m	10^{-4} m	5×10^{-10} $m^2\ s^{-1}$

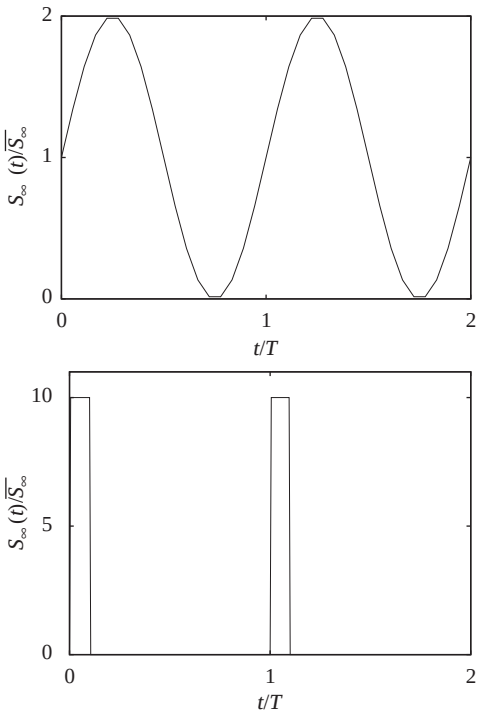

Fig. 2. Evolution of the two far-field signals used in transient simulations. For a given period T, the two signals differ in terms of the variance ratio $\sigma/\overline{S_\infty}^{-2} = 0.5$ for sine, $\sigma/\overline{S_\infty}^{-2} = 9$ for top-hat.

3. Results

Steady-state and transient simulations are presented in the following part of the work. The results of transient simulations (time-varying far-field concentration) are presented in terms of time-averaged normalized concentration gradients, as a function of the time-averaged far-field concentration $\overline{S_\infty(t)}$. In this work, two periodic signals are used for the far-field concentration, so a stationary periodic solution is finally obtained. These signals are shown in Fig. 2. The reason for this choice is to impose far-field signals with a marked difference in terms of variance in order to study the effect of the signal structure on the assimilation dynamics. Time averaging is performed over a full period once the stationary regime has been reached. When temporal evolutions are presented, the time is normalised by the diffusion time τ_D and the ratio $T^* = T/\tau_{\mathcal{D}}$ is used for a parametric study. This parameter compares the period, T, of the far-field concentration signal to the diffusion time. For small values of T^*, the far-field concentration changes faster than the time required for the concentration profile to get established. For large values of T^*, there is enough time for the concentration profile to get established between two concentration changes, so that a pseudo-steady-state approximation can be made.

3.1. Monod assimilation model at the cell interface

3.1.1. Constant far-field

A first set of calculations is performed with an imposed far-field concentration and the usual Monod equation at the cell

interface which corresponds to a Neumann boundary condition, see Eq. (4)

$$\varphi_{int} = \varphi_{max} \frac{S_{int}}{k_S + S_{int}}, \tag{16}$$

where S_{int} refers to the interfacial concentration and k_S is the half-saturation constant of the enzymatic reaction controlling assimilation at the cell–liquid interface. The results are presented in terms of normalised concentration gradients, $\varphi_{int}/\varphi_{max}$, as a function of the normalised far-field concentration S_∞/k_S. It can be reminded here that the normalised gradients are equivalent to the normalised uptake rates. In the present case, an analytical solution for the interfacial concentration and interfacial uptake rate can be found (see Appendix A). The resulting normalised uptake rate is shown by Fig. 3 with dashed lines. Note that identical results are obtained when solving the unsteady problem with the same boundary conditions. Since the results are plotted as a function of the bulk concentration S_∞, one observes that the half saturation is not obtained for $S_\infty/k_S = 1$ but for a higher value of the far-field concentration. The reason why the results are plotted against the bulk concentration is that in experimental situations the interfacial concentration is not measurable. If one dismisses the possible limitation by transport phenomena down to the cell scale, the uptake rate is directly computed from the bulk concentration. The corresponding uptake rate, $\varphi_{S_\infty}/\varphi_{max} = S_\infty/(k_S + S_\infty)$, is shown by Fig. 3 with solid lines. The comparison shows that significant differences can exist between the actual uptake rate and the values obtained neglecting the transport limitations. This discrepancy results from the concentration difference between the bulk and the microorganism surface. Such a situation is typical of an assimilation process taking place in the physical regime, when transport limits the assimilation rate. In case of severe transport limitation, an interfacial concentration close to zero can be reached as explained in Section 2.1. From the analytical solutions, it is possible to evaluate the difference between the uptake rate based on the far-field concentration and the actual uptake rate. This error is presented by Fig. 4 as a function of S_∞ for different k_S, and proves to be strongly dependent on the value of the half-saturation constant. For high values of k_S(10^{-3} kg_S m^{-3}) the deviation always remains lower than 5% whatever the bulk concentration. For small values of k_S (10^{-6} kg_S m^{-3}) the deviation can reach 100% of the maximum uptake rate when the bulk concentration lies in the range of 1–10 k_S. In the intermediate range of k_S, the maximum deviation is reached for far-field concentration equivalent to the half-saturation constant. Fig. 4 thus shows that, if the overall assimilation process is partly limited by the transport to the cell surface, then evaluating the uptake rate from the bulk concentration and a previously identified value of k_S (at the cell scale) leads to overestimate the actual uptake rate in the range $k_S \simeq \overline{S_\infty}$, especially for low k_S values. These results can also be analysed in the following way: let us consider $\varphi_{int} = f(\overline{S_\infty})$ (dashed line in Fig. 3) as an experimental data set from which the assimilation law has to be identified. This curve can be approximated using the Monod formulation

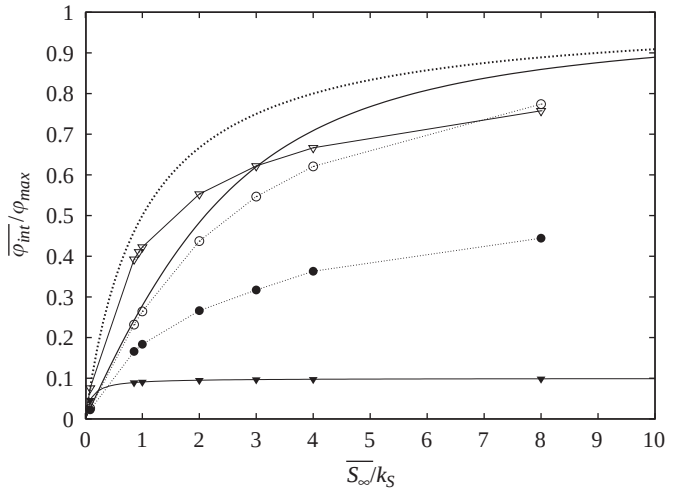

Fig. 3. Mean interfacial uptake rate as function of the normalised mean far-field concentration (results obtained with $k_S = 10^{-4}$ kg_S m^{-3}). Constant far-field: (· · · · · · · · ·), sine evolution: ○ and top-hat signal: • (both at $T^* \simeq 0.9$). Mean uptake rate based on the mean far-field concentration $\varphi(\overline{S_\infty})$: (——) and on the instantaneous far-field concentration $\overline{\varphi(S_\infty(t))}$ for sine: ▽ and top-hat: ▼.

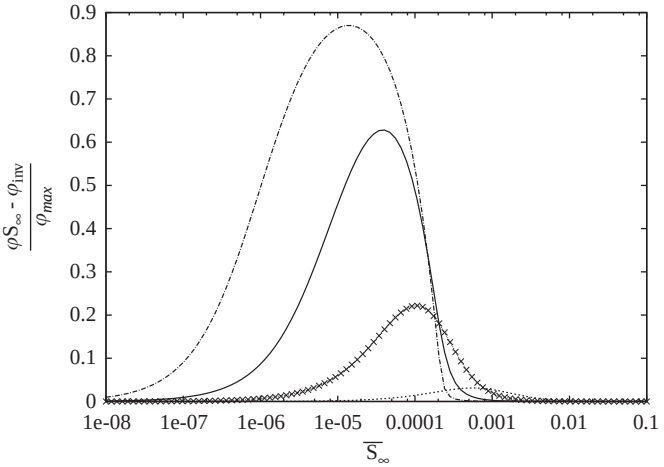

Fig. 4. Difference between the uptake rate based on the far-field concentration and the interfacial uptake rate for constant far-field concentrations at different affinity constants. $k_S = 10^{-6}$: (– · – · –), $k_S = 10^{-5}$: (——), $k_S = 10^{-4}$: (×) and $k_S = 10^{-3}$: (· · · · · · · · ·) (all affinity constants in kg_S m^{-3}).

$$\varphi = \varphi_{max} \frac{\overline{S_\infty}}{K_S + \overline{S_\infty}}, \tag{17}$$

and it leads to an apparent affinity constant K_S close to 2×10^{-4} kg_S m^{-3}. This value is different from that imposed in the calculations at the cell surface. It is therefore an apparent K_S which indeed reflects some transport limitation (purely physical phenomena). In other words, changing the efficiency of the mass transfer to the cell level can affect the identification of the apparent affinity constant K_S, even though the physics of the assimilation at the cell scale remains unchanged (same k_S).

3.1.2. Time-varying far field

Further calculations were performed with time-varying far-field concentration $S_\infty(L,t)$. Transient simulations are performed since there is no analytical solution in this case. The two types of signals shown by Fig. 2 were used. Both signals share the same period and the same mean far-field concentration. The results of numerical simulations for time-varying far-field concentration are examined in terms of time averages of the instantaneous interfacial uptake rate as defined in Eq. (16). Time-averaged values of the interfacial flux are reported in Fig. 3 for the particular case of $T^* = 0.9$ (line with circle). The main striking result is that, for a given mean far-field concentration, the assimilation rate differs when the surrounding medium is exposed to fluctuating concentrations. Moreover, comparing the sine and top-hat signals, the resulting assimilation rate is influenced by the structure of the far-field signal. This result suggests that, not only the mean concentration, but also the variance has an influence on the assimilation process. As already mentioned in

the previous section, the interfacial concentration is hardly accessible in practical situations. It is therefore interesting to examine the consequences of using the far-field concentration for the prediction of the uptake rate (k_S is assumed to be known). Two different situations occur. If the concentration fluctuations are measurable, a possible approach is to perform a time average of the instantaneous uptake rates evaluated from the instantaneous far-field concentrations (line with ∇ in Fig. 3):

$$\overline{\varphi(S_\infty(t))} = \varphi_{max}\overline{\frac{S_\infty(t)}{k_S + S_\infty(t)}}. \tag{18}$$

If the concentration fluctuations are filtered by the measuring probe, the only information available is the mean far-field concentration $\overline{S_\infty}$. So one can only evaluate the mean uptake rate from the mean far-field concentration through the following equation:

$$\varphi(\overline{S_\infty}) = \varphi_{max}\frac{\overline{S_\infty}}{k_S + \overline{S_\infty}}. \tag{19}$$

When this latter approach is used, the same results are obtained for both signals (because of identical $\overline{S_\infty}$, whatever the period or the variance) and they correspond to those for the constant far-field case at the same S_∞ (solid line, Fig. 3). In both situations, the prediction of the mean uptake rate is not correct. In Eq. (19) the temporal variations of the far-field concentration are not taken into account. In Eq. (18) the instantaneous uptake rate is algebraically linked to the far-field concentrations, which indeed reflects an immediate change of the uptake rate in response to a change in the far-field concentration. The real uptake rate lies in between.

Similar to what was proposed in the previous section, one can try and estimate the parameter of the assimilation law. Indeed, whatever the type of signal, a hyperbolic relationship is observed between the mean uptake rate and the mean far-field concentration. Therefore it is still possible to correlate the mean uptake rate to the mean far-field concentration, but the affinity constant is only an apparent K_S and reflects to a certain extent the existence of physical transport limitation. Here again, the identified value for K_S is higher that the actual k_S controlling the assimilation at the cell surface. For the same period of the fluctuations, it is also dependent on the type of signal.

3.2. First limitations

3.2.1. Limitations of the standard assimilation model

From numerical experiments it was shown that the apparent affinity constant K_S coming out from a data fitting of $\varphi = f(\overline{S_\infty})$ using a Monod expression is an apparent constant which can, in some cases, be affected by the existence of transport limitations and/or temporal concentration fluctuations. This constitutes an extension of the work of Merchuk and Asenjo (1995) that was limited to a constant assimilation rate (zero-order reaction at the cell surface). As a result, the apparent affinity constant was found to depend on the rate of transport only. In the present study, it is shown that the apparent affinity constant can reflect both biological and physical effects. Beyond the fact that cells are known to modify their affinity for the substrate using different type of transporters (Ferenci, 1999), this part of the work gives a physical explanation for the difficulty in identifying the parameter K_S. Consequences are twofold:

1. From an experimental point of view it questions the identifiability of the affinity constant. In the biological regime, the concentration at the cell surface is similar to the bulk concentration. Therefore a real k_S is identifiable from experiments. Apart from this biological regime, a concentration gradient between the microorganism and the bulk develops because of the competition between the rate of transport and the rate of assimilation. However it is still possible to relate the uptake rate to the bulk concentration through a standard Monod equation, but the parameters are actually affected by the operating conditions of the experiment. In particular, the rate of transport is dependent on the mixing efficiency in the bioreactor.
2. From a modelling point of view, the calculation of the mean interfacial uptake rate $\overline{\varphi_{int}}$ based on the far-field concentration $\varphi(\overline{S_\infty})$ is correct in the biological regime only since $S_{int} \simeq S_\infty$ and $K_S \simeq k_S$. But if assimilation does not proceed in the biological regime, the correct calculation of the uptake rate requires the transport to be solved down to the cell scale. The error in the calculation of the uptake rate based on the far-field concentration increases when k_S decreases. The smaller the affinity constant, the bigger the error on the uptake rate. In most modelling works, a predefined Monod law is used to quantify substrate assimilation in bioreactors, irrespective of a possible limitation by physical transport.

Although this demonstration was conducted considering a purely diffusive transport, the same conclusions are expected if a convective motion around the cell is present. This would modify the expression for the transport rate, but the dependance of K_S on the Damköhler number would remain. This suggests that mixing at the micro-scale can influence the assimilation, which is indeed confirmed by experiments (Dunlop and Ye, 1990). It will now be shown that the reference to an affinity constant is not necessary to predict the assimilation rate from the bulk concentration.

4. A new assimilation model for microorganisms in a substrate-limiting medium

4.1. Substrate assimilation model

Many experimental observations indicate that the so-called substrate limiting conditions are indeed situations where assimilation takes place in the physical regime. Lendenmann and Egli (1998) found that the uptake rate of *Escherichia coli* cells initially cultivated in a chemostat and then transferred in a substrate-rich medium was indeed constant, approximately equal to two thirds of the maximum uptake rate in batch culture and independent of the dilution rate in the chemostat. Neubauer et al. (1995) showed that after a prolonged starvation (27 min), the specific uptake rate of *E. coli* cells suddenly exposed to high substrate concentration could be an order of magnitude higher than the maximum uptake rate measured in a batch culture. Natarajan and Srienc (1999) found that the uptake rate of *E. coli* cells cultivated in a chemostat and then transferred into a substrate-rich medium was independent of the previously experienced dilution rate. All these results show that cells grown under substrate limiting conditions are potentially able to uptake the substrate at a higher rate. In fact, they actually do so as soon as they encounter more favourable conditions. This demonstrates that assimilation was previously taking place in the physical regime.

It is therefore proposed to consider that assimilation is either limited by the transport to the cell level or by the maximum uptake capacity of the cell. These two independent ideas are necessary to establish the model. In our case, diffusion controls the transport towards the cell surface. It will be shown that this choice does not limit the extent of our conclusions. The maximum uptake rate is assumed to be constant and given by Eq. (11). Steady and unsteady simulations will be performed and the results compared to those obtained with a standard Monod model.

4.2. Imposing boundary conditions

The choice of this assimilation model results in the setting of a specific boundary condition at the cell–liquid interface. This clearly appears if one considers these following asymptotic behaviors.

- *Non-limited culture*: By definition, this suggests that the uptake rate is maximum. Then, a fixed flux (Neumann boundary condition) corresponding to the maximum uptake rate is imposed.
- *Limited culture*: The mass flux at the cell interface is lower than the maximum uptake capacity. Then, one can assume that the interfacial concentration is constant and almost zero (Dirichlet boundary condition).

If a constant far-field concentration is set, the type of boundary condition to be used is uniquely determined by the values of φ_{max} and S_∞ as it will be shown in the following section. If a time-varying far-field concentration is imposed, one must consider the switch between the two boundary conditions. A so-called Robin boundary condition, which encompasses the case of Dirichlet and Neumann boundary conditions, is used at the microorganism surface $S(R,t)$. The switch between these two conditions is based on the value of the flux computed at the cell–liquid interface. Thus, the boundary condition is dynamically updated as the calculation proceeds depending on the instantaneous value of the interfacial mass flux.

4.3. Uniform environment

The focus was first put on the interfacial response for a constant far-field signal. This configuration mimics the medium surrounding a microorganism in a homogeneous macroscopical environment. Starting from a zero concentration field $S(r,0)=0$, a constant value is imposed at $S(r=L,t>0)=S_\infty$ and Eq. (2) is time-integrated until the steady state is reached. The transient behaviour of both the interfacial concentration and flux is not reported and is not of prime interest in the present work. The analytical solution for the transient case was used to validate the program. The results for different far-field concentrations are presented by Fig. 5. The normalised interfacial uptake rate, $\varphi_{int}/\varphi_{max}$, is plotted against the far-field concentration. The evolution of the interfacial flux is bilinear as a result of the imposed boundary condition at the cell surface. It is quite interesting to observe that this result resembles the Blackman bilinear model which gives the best fit for Koch and Houston Wang (1982) experimental data in the range of low concentrations. In this case the uptake rate can be expressed as a function of the far-field concentration: at low concentration, the interfacial concentration falls to zero and the flux is proportional to the far-field concentration as indicated in Eq. (7); above a saturation concentration S_∞^{sat} it becomes constant. This saturation concentration S_∞^{sat} corresponds to the limit case when $\varphi_{int}=\varphi_{max}$. Combining Eqs. (8) and (14), it comes:

$$S_\infty^{sat}\left(1+\frac{R}{L}\right)=\frac{\Phi_{max}}{4\pi DR}, \tag{20}$$

which simplifies into the following for $R \ll L$:

$$S_\infty^{sat}\approx\frac{\Phi_{max}}{4\pi DR}. \tag{21}$$

The far-field concentration below which a limitation of the uptake rate occurs is relatively low, but one must consider that the cell concentration is also very small. Indeed, in our modelling one cell occupies the centre of a sphere of diameter $L+R\simeq L$, thus the approximate corresponding cell concentration is given by $\rho_{cell}(R/L)^3$, i.e. 1 mg L^{-1}. It is not surprising that such a low concentration is required to limit such a small amount of cells. Adversely it also shows that defining a limiting concentration irrespective of the cell density is probably incorrect. Although it is not the central point of this paper, one can wonder if a normalised definition based on the ratio of the substrate concentration to the cell concentration would not be more appropriate to establish a comparison between various experimental data. In the present case we would get a ratio $S_\infty/X\simeq 10^{-1}$, for the switch between the diffusion-limited regime and the biological regime (assimilation rate limited by the assimilation capability of the cell).

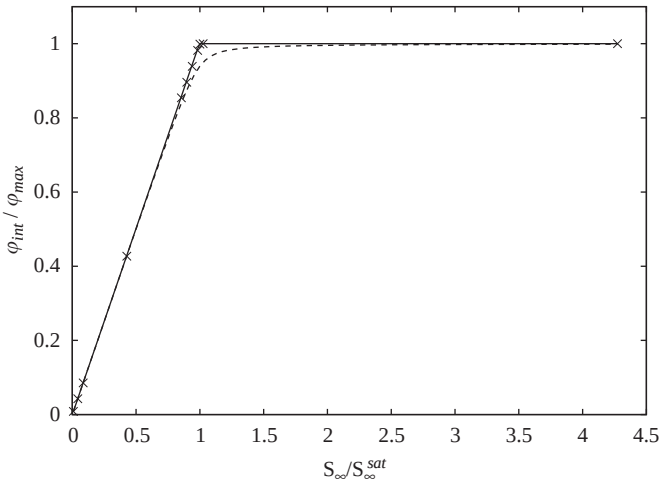

Fig. 5. Normalised interfacial uptake rate in the steady state for different constant far-field concentrations. (——) analytical solution, × numerical values extracted from the simulations. (· · · · · · · ·) numerical values using a Monod assimilation model with a high-affinity constant $k_S=10^{-6}$ kg_S m^{-3}.

Finally a short comparison with results for Monod assimilation model are given by Fig. 5 for a small affinity constant $k_S=10^{-6}$ kg_S m^{-3}. The results are very similar, encouraging the possibility to get rid of the macroscopic parameter K_S, especially if most of the substrate is assimilated by high-affinity transporters.

4.4. Time-varying far-field concentrations

A relationship between the far-field concentration and the uptake rate was found for a constant far-field. Is this also possible for time-dependent far-field concentration? In order to examine this point, a parametric study is performed on the ratio $T^*=T/\tau_{\mathcal{D}}$, where T is the period of the signal and $\tau_{\mathcal{D}}$ is the diffusional time. The parameters corresponding to each simulation are given in Tables 1 and 2. The far-field concentration is chosen so that over one period two sub-periods can be identified: one with the far-field concentration above the saturation concentration and the other one with the far-field concentration below the saturation concentration.

Fig. 6 shows the temporal evolutions of the concentration (dashed line) and the uptake rate (solid line) at the microorganism interface calculated with a top-hat far-field concentration signal (dotted line). The effect of the Robin-like boundary condition at the microorganism interface is visible: once the interfacial flux has reached its maximum value, the interfacial concentration rapidly increases. Adversely, when the cell is exposed to a severe limitation, the interfacial concentration falls down to zero first and the flux decreases afterwards. The logic of the switch can be explained considering a step-up of the far-field concentration followed by a step-down. As long as the flux reaching the cell surface is lower than the maximum uptake rate, a zero concentration boundary condition is used. Then, when the interfacial flux

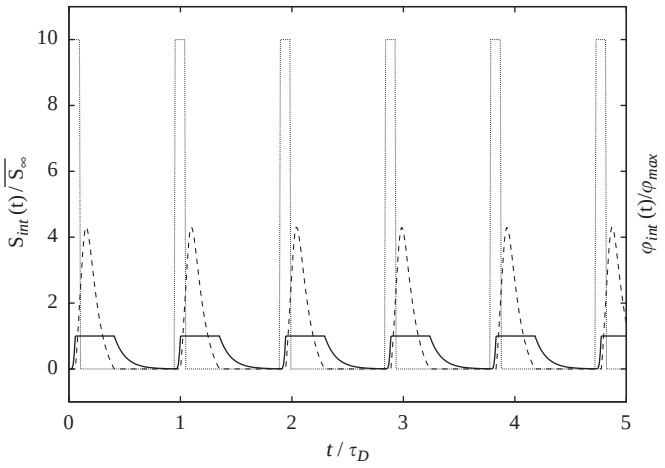

Fig. 6. Temporal evolution of the top-hat far-field concentration (· · · · · · · ·) and the corresponding interfacial concentration (– – – –) and interfacial uptake rate (——). $\overline{S_\infty} = 2 \times 10^{-4}$ kg$_S$ m^{-3}, $T^* \simeq 1.1$.

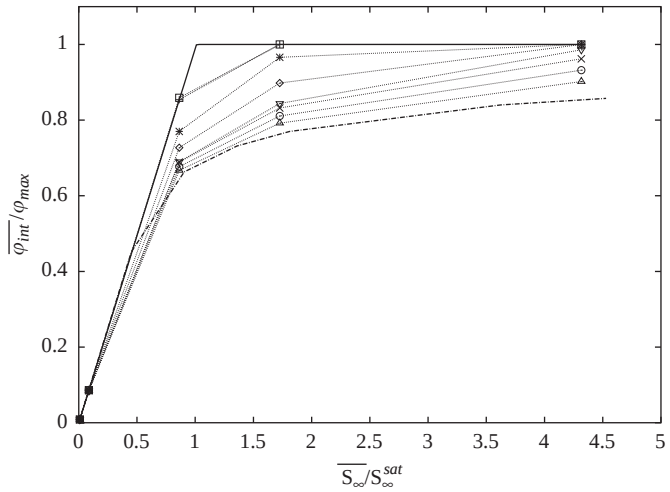

Fig. 7. Effect of characteristic timescale of the sine time-varying far-field concentration signal on the time-averaged interfacial uptake rate in the established state. (——) constant far-field, +: $T^* \simeq 0.1$, □: $T^* \simeq 0.2$, ≃: $T^* \simeq 0.5$, ◇: $T^* \simeq 0.7$, ▽: $T^* \simeq 0.9$, ×: $T^* \simeq 1.1$, ○: $T^* \simeq 1.4$, △: $T^* \simeq 2$, (– · – · –): $T^* \to \infty$ corresponding to the mean uptake rate based on the far-field concentration $\overline{\varphi(S_\infty(t))}$.

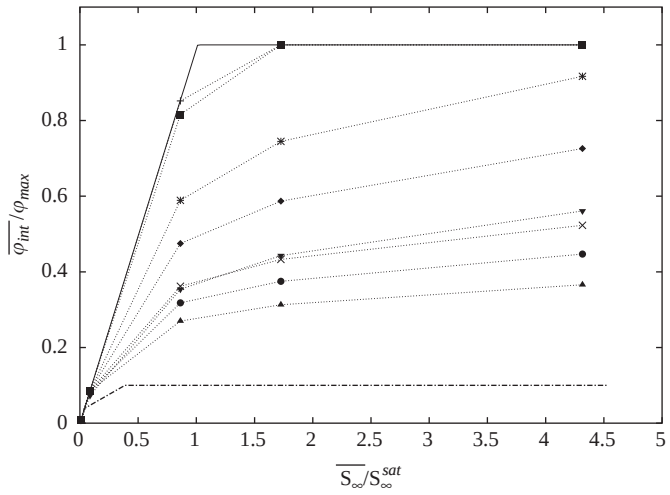

Fig. 8. Effect of characteristic timescale of the top-hat time-varying far-field concentration signal on the time-averaged interfacial uptake rate in the established state. (——) constant far-field, +: $T^* \simeq 0.1$, ■: $T^* \simeq 0.2$, ≃: $T^* \simeq 0.5$, ◆: $T^* \simeq 0.7$, ▼: $T^* \simeq 0.9$, ×: $T^* \simeq 1.1$, ●: $T^* \simeq 1.4$, ▲: $T^* \simeq 2$, (– · – · –): $T^* \to \infty$ corresponding to the mean uptake rate based on the far-field concentration $\overline{\varphi(S_\infty(t))}$.

equals the maximum uptake rate, a constant flux condition is imposed and the interfacial concentration progressively increases. Then, the far-field concentration falls suddenly. Shortly after, the interfacial concentration starts decreasing whilst the flux reaching the cell is unaffected (still maximum). In the end, the interfacial concentration reaches zero and it is no longer possible to internalize the substrate at the maximum uptake rate because transport towards the cell is limiting. So, a zero-concentration boundary condition is applied and the interfacial flux also starts decreasing.

It can be noticed that the interfacial concentration and flux variations are interdependent but not strictly correlated. The concentration at the cell interface $S_{int}(t)$ varies whilst the interfacial flux φ_{int} is constant and maximum. Inversely the interfacial uptake rate can vary while the related interfacial concentration remains zero. The duration of those events is expected to change with the far-field signal (period and structure).

Considering this fact, we decided to investigate in more detail the complex relationship between the structure of the far-field signal and the resulting interfacial signals. A sensitivity analysis on the influence of T^* on assimilation is conducted. Small values of T^* indicate that the concentration far from the cell changes rapidly in comparison with the time required to bring the substrate to the cell surface by diffusion. In this case, a direct relationship between the uptake rate and the far-field concentration can be established: the fluctuations of the far-field signal are actually filtered by the diffusion process and the resulting mean interfacial uptake rate is given as follows, based on Eq. (8):

$$\varphi_{int} \simeq \frac{\overline{S_\infty}}{R}. \tag{22}$$

For large T^*, the concentration profile has enough time to get established before the far-field concentration changes. Therefore, a quasi-steady-state hypothesis can be used. The mean uptake rate can be estimated from the averaging of the instantaneous uptake rates computed from instantaneous far-field concentrations. In the intermediate case, a strong competition between fluctuations and transport takes place. The effect of these interactions on the microorganism uptake rate is not easily predictable. In order to analyse the influence of the far-field concentration variation on assimilation, the time-averaged values of the interfacial flux are plotted against the mean far-field concentration for various T^* ratios. The results obtained with the sine and top-hat signals are presented by Figs. 7 and 8 respectively. The consequences of concentration fluctuations in the environment of the microorganism on the mean uptake rate are significant. Indeed, for a given mean far-field concentration, the mean normalised uptake rate in presence of concentration fluctuations is lower than that obtained in a uniform environment. A first consequence of the inhomogeneous concentration field is a decrease in the uptake rate of the cell.

At first sight, this conclusion seems to be in contradiction with the conservation of mass. The mean concentration is the same for all simulations, so where is the substrate which was not assimilated? In fact, one must remember that diffusion operates in two directions: it can bring the substrate towards the cell, or it can take it away from the cell if the substrate concentration at the cell surface is higher than that far from the cell. This is what happens, especially in the case of a top-hat signal because the pulse of high concentration is followed by a zero concentration period. Thus, the effects are much more pronounced for the top-hat signal than for a sine (see Figs. 7 and 8). The substrate which is not assimilated vanishes in the far field and it is lost for the cell

under consideration. One can observe that the cell was unable to internalize the substrate more rapidly despite the concentration peak because it has already reached its maximum uptake rate. It is remarkable to observe that this particular observation indicates that cells would take advantage of being able to increase their substrate uptake capacity. During the starvation period this additional capacity would remain unexploited, but it would allow them to uptake large amounts of substrate during the period of feast. A comparison between Figs. 7 and 8 shows that the higher the variance of the signal, the smaller the mean interfacial uptake rate. These can be regarded as the consequences of the competition between the assimilation and the mixing processes. Thus our simulations prove that the microorganism assimilation behaviour is strongly dependent on the mixing state of the surrounding medium. Despite the fact that the assimilation law at the cell level does not obey to a Monod equation, the averaged assimilation could be fitted with a Monod equation while both φ_{max} and K_S would depend on the characteristics of the far-field signal. In other words, the relationship between the observed uptake and the mean concentration might obey a Monod equation. But this is a macroscopic observation which reflects the interaction between transport phenomena and assimilation at the cell scale.

5. Discussion

The prediction of the substrate uptake rate is of crucial importance in modelling bioreactors because it couples the liquid phase to the biological reactions. Once the uptake rate is known, kinetic or metabolic models can be used to describe the intracellular reactions and the fate of the carbon within the cell. The concentration at the cell–liquid interface where assimilation actually takes place is not accessible through experiments, and it is therefore necessary to establish a relationship between the uptake rate and the average concentration in an elementary volume of fluid.

In most studies, experimental or numerical, dealing with fluid transport and biological reaction, the substrate consumption is ascribed to obey a general Monod law derived from macroscopic observations (Al-Homoud and Hondzo, 2008; Schmalzriedt et al., 2003; Lin et al., 2001). The survey of the literature reveals that the two constants used in this law are indeed dependent on the culture conditions (Lendenmann and Egli, 1998; Lin et al., 2001), which is obviously detrimental to the predictive capacities of the whole model. It was also found that different parameters are identified for the same strain (Koch and Houston Wang, 1982). The exact identification of these constants from experimental data is made difficult because of the strong interactions between assimilation and mixing taking place in bioreactors.

These considerations motivated the present work which aims at enlightening this scientific issue. It was decided to perform numerical simulations in a simplified case by taking into account only two well identified phenomena: mass transport and assimilation at the cell scale. One important thing to observe is that these two phenomena happen consecutively. Therefore, the observed rate results from the combination of both effects. In this paper, our choice was to solve directly the diffusive mass transport of substrate down to the cell level. Assimilation was described at the cell surface using two different assimilation laws (hyperbolic Monod and bilinear model). Thus these models correspond to the true biological uptake rate which is achieved without transport limitation. According to our simulation results, a hyperbolic relationship between the uptake rate and the mean concentration is systematically observed. But the effective affinity constant is clearly dependent on the physics of substrate transport. This conclusion stands for the two investigated models. The parameters of the hyperbolic relationship can be identified in the following cases:

- the imposed substrate concentration is constant $\varphi = \varphi(S_\infty)$,
- the characteristic time of transport is small compared to that of concentration changes ($T^* \ll 1$), leading to a quasi-steady state $\overline{\varphi} = \overline{\varphi(S_\infty(t))}$,
- the characteristic time of transport is very large compared to that of concentration changes ($T^* \gg 1$), resulting in a filtering of high frequencies $\overline{\varphi} = \varphi(\overline{S_\infty})$.

In order to perform this identification, the rate of transport has to be known and one must then solve the continuity of mass fluxes at the cell interface. An example is provided in the case of diffusion-controlled transport and a Monod assimilation law. It was found that the apparent affinity constant is only dependent on the rate of transport. For the intermediate cases ($T^* \approx 1$) the relationship between the uptake rate and the mean concentration still obeys a hyperbolic equation, but the affinity constant is now also impacted by the ratio T^*. In that case, it was observed that the temporal characteristics of the interfacial uptake rate and concentration are decoupled from those of the far-field signal. Moreover they also depend on the type of signal itself (mean value and variance). This is illustrated by Fig. 6. It is particularly interesting to observe that for a top-hat signal with a mean value corresponding to a non-limiting concentration ($\overline{S_\infty} > S_\infty^{sat}$), the interfacial concentration periodically falls down to zero and the uptake rate is not maximum. Moreover the duration of these events (zero concentration and sub-optimal uptake rate) is impacted by the time constant ratio as shown by Fig. 9. The same kind of observations can be made for a sine evolution of the far-field concentration and they are not restricted to a particular type of assimilation model. This suggests that cells may locally be exposed to starvation whereas the mean concentration is above the supposed limiting value.

This model developed for purely diffusive transport aimed at analysing the behaviour of cells in bioreactors. Further development can be envisaged with a more realistic configuration for the substrate transport. Indeed, numerous studies of heat and mass transfer rates from spherical particles immersed in low-Reynolds-number velocity fields have been performed over the years (Acrivos and Taylor, 1962; Frankel and Acrivos, 1968). Theoretical analyses have led to the development of asymptotic expressions for the Nusselt or Sherwood numbers as a function of the Péclet

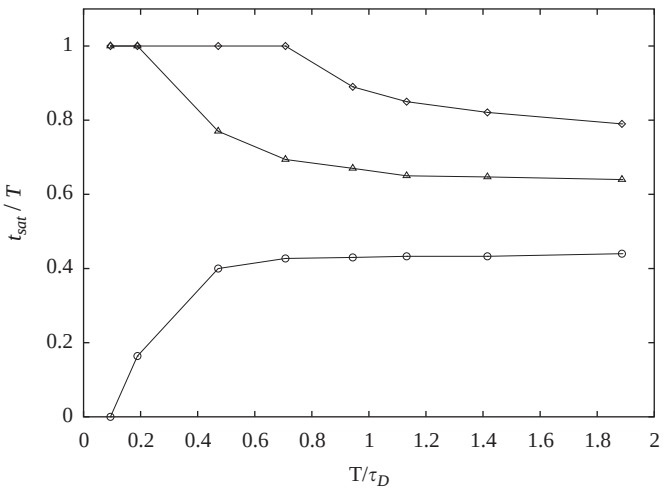

Fig. 9. Saturation time at the maximum uptake rate over the corresponding period, in function of the characteristic time ratio for the sine far-field signal. ◇: $\overline{S_\infty}/R\varphi_{max} = 4.3$, △: $\overline{S_\infty}/R\varphi_{max} = 1.7$, ○: $\overline{S_\infty}/R\varphi_{max} = 0.85$.

number Pe for the cases of uniform to simple shear flow at infinity. For small Péclet numbers, the diffusion effects are dominant near the particle but an additional transfer, due to convection effects at large distance from the particle, enhances the purely diffusive mass transfer rate Sh_0 and the added non-dimensionalized transfer rate is equal to $\alpha Sh_0 Pe^{1/2}$. At large Péclet numbers the transfer rate depends on the velocity distribution at the particle (Poe and Acrivos, 1976), and can be either a constant or depending the Péclet number as $\beta Pe^{1/2}$. Batchelor (1980) later derived a general method to determine the numerical values of the constants α and β for different given types of shear flow. The usual transfer rate from the particle to the surrounding medium is studied, but previous studies (Purcell, 1978) have shown that results are similar for mass transfer towards a particle. Further numerical studies (Feng and Michaelides, 2000) concern the transient heat transfer from a spherical particle at high Reynolds and Péclet numbers, and three-dimensional simulations could be envisaged in order to account for shear flow around the micro-organism and substrate transport and assimilation. Considering the previous results for convective flows, in comparison with diffusive transport, smaller characteristic time scales are expected for convective transport on the domain length L. Nevertheless, the overall conclusions would remain unaffected.

These conclusions help in understanding the experimental results of Garcia et al. (2009) showing that GFP (Green Fluorescent Protein) reporting strains sensitive to oxygen limitation were illuminated whilst cultivated in an agitated bioreactor with the DO (Dissolved Oxygen) maintained above 20%. It is known that starvation activates high-affinity transporters (Ferenci, 1999). Transposing the observations of Garcia and co-workers to the glucose assimilation, one can also imagine that the repeated exposure of cells to low-concentration events can activate high-affinity transporters even if the measured substrate concentration is above the limiting value. This would partly explain the extra-assimilation capacity observed in poorly micro-mixed industrial bioreactors and the failure of standard models to accurately predict both the assimilation rate and the amount of over-flow metabolites. Ferenci (1999) observed that, in a batch culture, the gene coding for the high-affinity transporters are activated at relatively high substrate concentration ($60\ \mathrm{mg\ L^{-1}}$), much higher than K_S ($\sim 1\ \mathrm{mg\ L^{-1}}$). Under these conditions it is difficult to understand the triggering factor for gene activation: the substrate influx is not limiting and the concentration is far above the affinity constant K_S. Considering the present work, one can analyse the experimental data in a slightly different way. First of all, the substrate concentration is not the accurate quantity; one must rather follow the ratio of the substrate to cell concentration S/X which can be regarded as the ratio between the transport rate $\mathcal{D}_m(S-Si)/L$ and the assimilation rate μ_X by the cell. In the exponential growth phase, μ is constant. The rate of transport is also constant if the agitation speed is maintained. As the batch culture proceeds, the substrate concentration decreases and the amount of cells increases, so the ratio S/X progressively decreases indicating that transport limitation is more and more likely to occur. From the cell point of view, it means that the interfacial concentration is also progressively falling down to zero. When this lower value is reached, it can surely be considered as a signal for activating high-affinity transporter. Our results show that the uptake flux can be maximal while the far field concentration is high above K_S and the interfacial concentration is close to zero. Insel et al. (2007), have shown that the initial substrate to microorganism ratio directly influence the population growth in batch cultures. By setting constant both the mean cell residence time and the top-hat feed, they observed the kinetic response of *E. coli*. A regulation of growth metabolism by decreasing the maximum growth rate and increasing the substrate affinity constant results in a higher assimilation capacity.

Finally, in the conclusion of their work, Schmalzriedt et al. (2003) pointed out two directions for future improvements: dynamic metabolism modelling and micro-mixing. The former point has been addressed by Lapin et al. (2004). The experimental evidence of micro-mixing issues in biological reactors was brought some years ago by Dunlop and Ye (1990) and Amanullah et al. (2001). In the field of chemical-reactor engineering, the term micro-mixing is used to depict the situation where the characteristic mixing time is similar or lower than the characteristic reaction time. When mixing competes with the reaction a concentration distribution occurs, so that homogeneity down to the molecular scale is not achieved in the reactor. The concentration distribution within the volume of control results from the combined effects of mixing and reaction. If the relationship between the reaction rate and the concentration is not linear, the actual average reaction rate differs from the reaction rate based on the average concentration. Since Eq. (1) is not linear one can effectively suspect that biological reactions (and substrate assimilation in particular) may lead to micro-mixing issues.

6. Conclusion

In this work a dynamic model for the assimilation of substrate by a microorganism subjected to concentration variations in its micro-environment is proposed. The transport of substrate towards the cell is represented by a purely diffusive process. Different assimilation models were scrutinised at the micro-organism interface. These models result in specific boundary conditions at the micro-organism interface. Firstly a classical Monod assimilation model was used, assuming the maximum specific growth rate and the affinity constant to be known. As expected a hyperbolic relationship between the uptake rate and the mean far-field concentration is found, but different effective affinity constants are observed depending on whether transport limits assimilation or not. An alternative model for substrate assimilation was developed in order to get rid of this parameter. The only biological parameter needed in this second approach is the maximum specific growth rate, from which the maximum interfacial mass flux can be estimated. A specific time-varying boundary condition, based on the substrate flux at the cell surface, is set. The results were similar to those obtained with a standard Monod law: a general hyperbolic evolution for the uptake rate is obtained for various far-field signal evolutions. However it was shown that the results differ depending on the type of fluctuations imposed in the microenvironment of the cell. This supports the idea that if assimilation takes place in the physical assimilation regime (the transport limits the assimilation) the uptake rate can not be directly derived from the biological assimilation. Finally, it was shown that the magnitude and duration of critically low-concentration events (at the cell surface) are dependent on the concentration fluctuations to which the cell is submitted. In that sense this work is helpful in understanding how the concentration fluctuations in the microenvironment of cells (caused by imperfect mixing at the cell level) may be responsible for the activation of high-affinity transporters.

Nomenclature

Latin letters

a_c	cell surface, $\mathrm{m^2}$
$\mathcal{D}$	molecular diffusivity, $\mathrm{m^2\ s^{-1}}$
k_S	half saturation constant at the cell interface, $\mathrm{kg_S\ m^{-3}}$
K_S	macroscopic affinity constant for the substrate S, $\mathrm{kg_S\ m^{-3}}$
L	length of the computational domain, m
m_c	cell mass, $\mathrm{kg_S}$

q_S specific uptake rate, $kg_S\ kg_X^{-1} s^{-1}$
r radial coordinate, m
R microorganism radius, m
S substrate concentration, $kg_S\ m^{-3}$
T period of the far-field signal, s
T^* non-dimensioned time ratio
Y_{XS} conversion yield of substrate into biomass, $kg_X\ kg_S^{-1}$

Non-dimensional numbers

Pe Péclet number
Re Reynolds number
Sh Sherwood number
Sh_0 purely diffusive mass transfer rate

Greek letters

α constant
β constant
ε dissipation rate, $m^2\ s^{-3}$
ρ_{cell} cell density, $kg_X\ m^{-3}$
μ specific growth rate, s^{-1}
φ substrate flux, $kg_S\ m^{-4}$
Φ mass flux, $kg_S\ s^{-1}$
σ variance, s^2
$\tau_{\mathcal{D}}$ diffusional time, s

Subscripts and superscripts

$\langle \cdot \rangle$ spatial average
$\bar{\cdot}$ time average
$\cdot_{int}$ interfacial
$\cdot_{\infty}$ far-field
$\cdot_{max}$ maximal
$\cdot_{sat}$ saturation

Appendix A. Analytical solution for 1D spherical diffusion equation with Monod assimilation model

In the steady state, the radial component of the spherical diffusion equation yields:

$$\frac{\partial}{\partial r}\left(r^2\frac{\partial S}{\partial r}\right)=0. \tag{A.1}$$

Using the Monod assimilation model the boundary conditions for the problem are:

- Constant far-field concentration:
$$S(r=R+L)=S_\infty \tag{A.2}$$

- Constant assimilation at the cell interface:
$$\left.\frac{dS}{dr}\right|_{r=R}=\varphi_{max}\frac{S_{int}}{k_S+S_{int}} \tag{A.3}$$

The substrate concentration in the domain is

$$S(r)=S_\infty+R^2\varphi_{max}\frac{S_{int}}{k_S+S_{int}}\left(\frac{1}{R+L}-\frac{1}{r}\right) \tag{A.4}$$

At $r=R$ the interfacial concentration yields:

$$S(r=R)=S_{int}=S_\infty+R^2\varphi_{max}\frac{S_{int}}{k_S+S_{int}}\left(\frac{1}{R+L}-\frac{1}{R}\right), \tag{A.5}$$

leading to a second-order equation for the interfacial concentration S_{int}. The positive solution finally gives S_{int} as a function of R,L,k_S,S_∞

$$S_{int}=\frac{1}{2}\left(-\left(k_S-S_\infty+\frac{RL}{R+L}\varphi_{max}\right)\right)+\frac{1}{2}\left(\sqrt{\left(k_S-S_\infty+\frac{RL}{R+L}\varphi_{max}\right)^2+4k_SS_\infty}\right), \tag{A.6}$$

and the interfacial uptake rate is given by

$$\varphi_{int}=\varphi_{max}\frac{S_{int}}{k_S+S_{int}} \tag{A.7}$$

References

Acrivos, A., Taylor, T., 1962. Heat and mass transfer from single sphere in Stokes flow. Phy. Fluids 5, 387–394.
Al-Homoud, A., Hondzo, M., 2008. Enhanced uptake of dissolved oxygen and glucose by *Escherichia coli* in a turbulent flow. Appl. Microbiol. Biotechnol. 79 (4), 643–655.
Amanullah, A., McFarlane, C.M., Emery, A.N., Nienow, A.W., 2001. Scale-down model to simulate spatial pH variations in large-scale bioreactors. Biotechnol. Bioeng. 73 (5), 390–399.
Bajpai, R.K., Reuss, M., 1982. Coupling of mixing and microbial kinetics for evaluating the performance of bioreactors. Can. J. Chem. Eng. 60, 384–392.
Batchelor, G., 1980. Mass transfer from small particles suspended in turbulent fluid. J. Fluid Mech. 98, 609–623.
Bylund, F., Collet, E., Enfors, S.-O., Larsson, G., 1998. Substrate gradient formation in the large-scale bioreactor lowers cell yield and increases by-product formation. Bioprocess Biosyst. Eng. 18, 171–180.
Chassagnole, C., Noisommit-Rizzi, N., Schmid, J.W., Mauch, K., Reuss, M., 2002. Dynamic modeling of the central carbon metabolism of *Escherichia coli*. Biotechnol. Bioeng. 79 (1), 53–73.
Dunlop, E.H., Ye, S.J., 1990. Micromixing in fermentors: metabolic changes in *Saccharomyces cerevisiae* and their relationship to fluid turbulence. Biotechnol. Bioeng. 36 (1), 854–864.
Enfors, S.O., Jahic, M., Rozkov, A., Xu, B., Hecker, M., Jürgen, B., Krüger, E., Schweder, T., Hamer, G., O'Beirne, D., Noisommit-Rizzi, N., Reuss, M., Boone, L., Hewitt, C., McFarlane, C., Nienow, A., Kovacs, T., Trägårdh, C., Fuchs, L., Revstedt, J., Friberg, P.C., Hjertager, B., Blomsten, G., Skogman, H., Hjort, S., Hoeks, F., Lin, H.Y., Neubauer, P., van der Lans, R., Luyben, K., Vrabel, P., Manelius, Å., 2001. Physiological responses to mixing in large scale bioreactors. J. Biotechnol. 85 (2), 175–185.
Feng, Z.-G., Michaelides, E.E., 2000. A numerical study on the transient heat transfer from a sphere at high Reynolds and Péclet numbers. Int. J. Heat Mass Transfer 43, 219–229.
Ferenci, T., 1996. Adaptation to life at micromolar nutrient levels: the regulation of *Escherichia coli* glucose transport by endoinduction and camp FEMS. Microbiol. Rev. 18 (4), 301–317.
Ferenci, T., 1999. Regulation by nutrient limitation. Curr. Opinion Microbiol. 2, 208–213.
Frankel, N.A., Acrivos, A., 1968. Heat and mass transfer from small spheres and cylinders freely suspended in shear flow. Phy. Fluids 11, 1913–1918.
Garcia, J., Cha, H., Rao, G., Marten, M., Bentley, W., 2009. Microbial nar-GFP cell sensors reveal oxygen limitations in highly agitated and aerated laboratory-scale fermentors. Microb. Cell Factories 8, 6.
Hansford, G.S., Humphrey, A.E., 1966. The effect of equipment scale and degree of mixing on continuous fermentation yield at low dilution rates. Biotechnol. Bioeng. 8, 85–96.
Hondzo, M., Al-Homoud, A., 2007. Model development and verification for mass transport to *Escherichia coli* cells in a turbulent flow. Water Resour. Res. 43.
Insel, G., Celikyilmaz, G., Ucisik-Akkaya, E., Yesiladali, K., Cakar, Z., Tamerler, C., Orhon, D., 2007. Respirometric evaluation and modeling of glucose utilization by *Escherichia coli* under aerobic and mesophilic cultivation conditions. Biotechnol. Bioeng. 96, 94–105.
Koch, A.L., Houston Wang, C., 1982. How close to the theoretical diffusion limit do bacterial uptake systems function? Arch. Microbiol. 131 (1), 36–42.
Lapin, A., Muller, D., Reuss, M., 2004. Dynamic behavior of microbial populations in stirred bioreactors simulated with Euler–Lagrange methods: traveling along the lifelines of single cells. Ind. Eng. Chem. Res. 43 (16), 4647–4656.
Lara, A.R., Galindo, E., Ramírez, O., Palomares, L., 2006. Living with heterogeneous bioreactors: understanding the effect of environmental gradients in cells. Mol. Biotechnol. 34 (3), 355–381.
Larsson, G., Törnkvist, M., Wernersson, E., Trägårdh, C., Noorman, H., Enfors, S., 1996. Substrate gradients in bioreactors: origin and consequences. Bioprocess Biosyst. Eng. 14 (6), 281–289.
Lendenmann, U., Egli, T., 1998. Kinetic models for the growth of *Escherichia coli* with mixtures of sugars under carbon-limited conditions. Biotechnol. Bioeng. 59 (1), 99–107.

Lin, H.Y., Mathiszik, B., Xu, B., Enfors, S.-O., Neubauer, P., 2001. Determination of the maximum specific uptake capacities for glucose and oxygen in glucose-limited fed-batch cultivations of *Escherichia coli*. Biotechnol. Bioeng. 73 (5), 347–357.

Merchuk, J.C., Asenjo, J.A., 1995. The Monod equation and mass transfer. Biotechnol. Bioeng. 45 (1), 91–94.

Namdev, P.K., Thompson, B.G., Gray, M.R., 1992. Effect of feed zone in fed-batch fermentations of *Saccharomyces cerevisiae*. Biotechnol. Bioeng. 40, 235–246.

Natarajan, A., Srienc, F., 1999. Dynamics of glucose uptake by single *Escherichia coli* cells. Metab. Eng. 1 (4), 320–333.

Natarajan, A., Srienc, F., 2000. Glucose uptake rates of single *E. coli* cells grown in glucose-limited chemostat cultures. J. Microbiol. Methods 42 (1), 87–96.

Neubauer, P., Häggström, L., Enfors, S.-O., 1995. Influence of substrate oscillations on acetate formation and growth yield in *Escherichia coli* glucose limited fed-batch cultivations. Biotechnol. Bioeng. 47 (2), 139–146.

Poe, G., Acrivos, A., 1976. Closed streamline flows past small rotating particles: heat transfer at high Péclet numbers. Int. J. Multiphase Flow 2, 365–377.

Purcell, E.M., 1978. The effect of fluid motions on the absorption of molecules by suspended particles. J. Fluid Mech. 84, 551–559.

Schmalzriedt, S., Jenne, M., Mauch, K., Reuss, M., 2003. Integration of physiology and fluid dynamics. In: von Stockar, U., van der Wielen, L., Bruggink, A., Cabral, J., Enfors, S.-O., Fernandes, P., Jenne, M., Mauch, K., Prazeres, D., Reuss, M., Schmalzriedt, S., Stark, D., von Stockar, U., Straathof, A., van der Wielen, L. (Eds.), Advances in Biochemical Engineering/Biotechnology, vol. 80. Springer, Berlin, Heidelberg, pp. 19–68.

Truskey, G.A., Yuan, F., Katz, D.F., 2004. Transport Phenomena in Biological Systems, 1st Edition Pearson Prentice Hall, NJ, Upper Saddle River.